The design of slushflow barriers: Laboratory experiments

Kristín Martha Hákonardóttir[1*] and Katrín Helga Ágústsdóttir[2]

[1] Verkís, Ofanleiti 2, IS-103 Reykjavík, ICELAND*
[1] University of Iceland, Faculty of Industrial Engineering, Mechanical Engineering and Computer Science, ICELAND
**Corresponding author, e-mail: kmh (at) verkis.is*

ABSTRACT

We report on a series of laboratory experiments to study the interaction of slushflows with catching dams. The aim of the experiments is to identify an engineering design that effectively stops a slushflow upstream of a catching dam. In the experiments, we use water as a substitute for slush. The chute flow is scaled with the Froude number and the barrier height is scaled with the depth of the chute flow and the Froude number. We find high run-up (splash) and thus high impact forces may be inferred, during the initial impact of the flow with an impermeable barrier, resulting in overtopping of the dam. The splash is followed by semi-steady fountaining, with overflow until an abrupt transition to a hydraulic jump occurs and overtopping ceases. The high initial splash may be interpreted in terms of high pressures that develop during the impact due to the incompressibility of water as opposed to granular flow. We note the importance of reducing the initial splash to minimize overtopping and shorten the transition to a hydraulic jump state. A row of relatively low, steep braking mounds upstream of an impermeable, steep dam is extremely effective. We find that energy dissipation does not take place at the upstream mound face, but rather downstream from the mounds, due to turbulence. A permeable or partly permeable steep rock dam or a rock berm is also effective to reduce overtopping.

1. INTRODUCTION

Slushflows occur when water-saturated snowpack is mobilized. Slushflows are common in Norway, Iceland, Alaska, other Arctic regions, as well as in Japan, and may become more common in lower altitude Alpine regions, due to global warming. Erik Hestnes at the NGI in Norway has studied Norwegian slushflows for over three decades (Hestnes, 1985, 1998). In a recent paper, Hestnes and Kristensen (2011) identify three types of slushflows, based on the triggering mechanism: 1) Liquefaction of a wet snow slab, 2) release of a slab avalanche into an increasingly wetter snowpack and 3) avalanches into lakes.

The resulting flows may be highly turbulent and travel with steep flow fronts (see Figure 1), much like dam-break floods. Gude and Scherer (1998) studied slushflows in Spitsbergen and North Sweden. They used the Froude number of the flows to distinguish between minor, $Fr < 1$ and larger slushflows or slushtorrents, $Fr > 2$. Wave-like instabilities on the free surface have been observed for flows with Fr close to 1 (surges or roll waves, Sovilla et al., 2012) and more than one release from the same starting zone is common, with the lower part releasing first and the upper part following (Hestnes et al., 2011; Ágústsson et al., 2003b). The speed of large slushflows is generally lower than the speed of dry snow avalanches, which may be due to high basal resistance in the flow track. The flows generally entrain snow, soil and rocks on the way and the flowing mass increases substantially downslope.

Large slushflows may be highly destructive, exerting dynamic pressures on obstacles of the same order as large dry-snow avalanches.

The present study is motivated by the challenge of stopping slushflows above the villages of Patreksfjörður and Bíldudalur in Nortwestern Iceland. Residential houses are threatened by slushflows with volumes of 10–50 thousand cubic meters and both towns have been hit by slushflows from prominent gullies in the mountainsides (Ágústsson et al., 2003a; 2003b). A catastrophic slushflow was released above Patreksfjörður in January 1983, claiming three lives and damaging 16 houses, see Figure 1. Back calculations of flow speeds suggest a speed of the slushflow of 10 to 15 m/s (Jóhannesson and Hákonardóttir, 2004; Gauer, 2004). Channels to direct the flows through the residential area, to the ocean were proposed in earlier appraisal studies (Sigurðsson et al., 1998), thereby splitting the towns in two and removing several houses in the way. The proposals were rejected by the town council due to the undesired impact on the town's appearance. The channel in Patreksfjörður would also have cut access to the hospital from the western part of town, during and after a large slushflow. In 2015, Stefan Margreth of the SLF in Switzerland, was brought in for consulting. He recommended investigating the feasibility of a catching dam as an option for the protection of this part of the town, including detailed studies of the retarding effect of such structures against slushflows (Margreth, 2015). Hestnes and Sandersen (2000) discuss mitigation measures in the track of slushflows. They recommend catching dams to restrict the run-out of slushflows and breaking structures as used for retarding debris flows, for retarding the flows, upstream of the dams. They do not suggest stopping such flows.

Figure 1 A slushflow in Western Norway in May 2010 (Hestnes et al., 2011). A newspaper clip from Morgunblaðið of slushflow debris in Patreksfjörður, Northwestern Iceland in January 1983.

A few experimental studies on the velocity profile and viscosity of slushflows have been conducted (Jaedicke et al., 2008; Upadhyay et al., 2010). Jaedicke et al. (2008) additionally measured impact pressure on an obstacle in the flow path, measuring the highest pressures as the flow front hit the obstacles. Small scale experimental studies of granular flows have shown similarities between granular flows and shallow water flows and indicate that shallow-water theory may be directly applied to calculate phenomena such as shocks (hydraulic/granular jumps) in the interaction with obstacles (Savage, 1979; Brennen et al., 1983; Gray et al., 2003; Hákonardóttir and Hogg, 2005). Dissimilarities have also been observed in small scale experiments with water. Hákonardóttir and Hogg (2005) report on short-lived water jets moving up obstacle faces in the initial impact, with run-up or splashing exceeding the run-up calculated from energy conservation. This behaviour is not observed to the same extent in impacts of

granular flow with obstacles. The difference is ascribed to the incompressibility of water, whereas the granular flow front is dilute and compressible. Similar splashes may be observed in violent and destructive ocean wave impacts on harbour walls, see Figure 2.

Figure 2 Stay away from the seafront: Waves crash against the promenade in Aberystwyth, Wales, as strong winds and high tides continue in western Britain. Taken from the Daily Mail article 2534511.

The goal of the experiments presented in this paper is to identify an engineering design that effectively stops slushflows upstream of an approximately 10 m high catching dam, where a 1–3 m thick slushflow at the speed of 10–20 m/s may be expected (Froude number between 2 and 5). We draw upon experience in the design of dams and mounds for retarding dry-snow avalanches (Jóhannesson et al., 2009) of ocean breakwaters (van der Meer and Sigurðarson, 2017; Bruce et al., 2009; Najafi-Jilani and Monshizadeh, 2017), wave impact theory (Cooker and Peregrine, 1995), and the design of obstacles (baffle/chute blocks) in dam spillways and bottom outlets of hydropower plants to dissipate the energy of the flow (Peterka, 1984).

2. THEORY

2.1 Scaling

The Froude number of a free-surface flow, upstream of an obstacle, is an important dimensionless parameter which is given by

$$Fr^2 = \frac{u^2}{\mathrm{g}\, h \cos \xi}\,, \qquad (1)$$

where u is flow speed, h is flow depth and ξ is the slope angle. The Froude number is commonly used to scale free-surface fluid flow, if viscous effects are negligible. It measures the speed of the flow relative to the speed of the small-amplitude surface waves. Issler (2003) suggests that for dry-snow avalanches Fr is in the range 5 to 10. We find that the Froude number for large slushflows that may be expected in Patreksfjörður, Northwestern Iceland, is between 2 and 5 on the debris cone, where catching dams may be located (see discussion in section 1).

2.2 Splash

Hákonardóttir and Hogg (2005) observed pressure-induced splash in the initial impact of high Froude number water flows and dams. The splash height may be calculated from pressure impulse by Cooker and Peregrine (1995).

2.3 Energy conservation

The maximum run-up of a snow avalanche on a catching dam has traditionally been determined from point-mass energy conservation (Salm et al., 1990; Rudolf-Miklau et al., 2015).

2.4 Ballistic trajectories

Jets of fluid or granular flows over relatively low obstacles (H/h_1 = 1–5, where H is obstacle height) have in laboratory experiments been observed to follow ballistic trajectories.

2.5 Hydraulic jump

The flow depth for an upstream propagating hydraulic jump may be determined from classical analysis of two-dimensional hydraulic jumps, mass and momentum fluxes are conserved across the jump, but mechanical energy is dissipated (Hager, 1992). The hydraulic jump for flows with Froude numbers between 2.5 and 4.5 is unstable and oscillating. Dissipation of energy flux over the jump is 0.15 to 0.45 (Hager, 1992). Interestingly, the hydraulic jump for flows with Froude numbers between 1.7 and 2.5 is weak with series of small rollers.

3. EXPERIMENTAL SETUP AND DESIGN

Slushflows are a partly-saturated mixture of water and snow, with a range from almost pure water to very wet snow mixed with mud and rocks. We use water to study slushflows, since slush is hard to produce in a consistent manner and scale in the laboratory. By using water, we enhance the difference with granular flows and the interpretation of the results is simplified.

The experimental chute is approximately 9 m long and 1.2 m wide, with a 6 m^3 tank at the upstream end, 1.5 m higher than the horizontal part of the chute, see Figure 3. Water is released from the tank with a quick release valve, to imitate dam break. The system is based on the design of wave simulators, to recreate run-up of ocean waves on flood banks at a large scale (van der Meer, 2001). The valve is 1 m wide and 0.3 m high. Water is released from the tank onto a chute, with obstacles for testing on a level section near the end of the chute, see Figure 3.

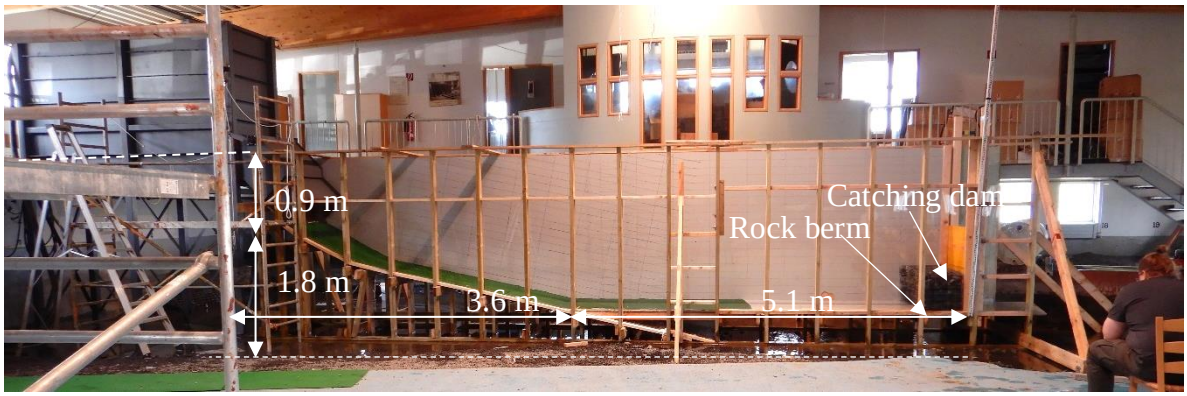

Figure 3 Setup C.6. The experimental chute is 9 m long and 1.2 m wide with a 6 m^3 tank.

3.1 Scaling

The experimental setup was designed based on Froude number scaling of the flow and length scaling of 1:10 (lab.:field), as is common in wave experiments (Bruce et al., 2009) and the following scaling arguments:

Viscous effects: The Reynolds number in these experiments is calculated to be approximately $3 \cdot 10^5$, which is sufficiently high that viscous effects may be neglected.

Froude number: Fr_1 = 3–5, as for large slushflows expected in Patreksfjörður (see section 1).

Flow depth: The flow depth is scaled by a factor of 10.

Dam height: $H_{\text{dam}} / h_2 > 1$, where h_2 is the depth of a stationary hydraulic jump.

Mound height: H_{mound} / h_1 = 2–3, based on experimental results of optimum mound heights in granular flows (Hákonardóttir et al., 2003b; 2003c).

The ratio of the width of the chute to the width covered by obstacles: B_{mounds}/b_{chute} = 0.5 and B_{dam}/b_{chute} = 1.

Rock size: $D_{\text{field}} = 10\, D_{\text{lab.}}$, where D is the diameter of rocks in the rock dams, to ensure scaling of impact forces vs. weight (horizontal resistance) and void ratio. The rock size scaling is derived from Froude number scaling and the ratio of the force due to dynamic pressure and a resistance force, proportional to the weight of the rocks.

Flow speed: $u_{\text{field.}} = 10^{1/2}\, u_{\text{lab.}}$, derived from the Froude number and flow-depth scaling).

Time: $t_{\text{field.}} = 10^{1/2}\, t_{\text{lab.}}$.

3.2 Dam setup and experimental procedure

In each experiment, the tank is filled up to a depth of 0.9 m and 2.7 m^3 of water released instantaneously onto the chute. The vertical drop from the initial water level onto the horizontal chute section is 2.7 m.

The flow speed on the chute was measured at three locations, upstream of the obstacles as a function of time, using a A-Ott C31 propeller current meter (relative accuracy ±2%). The flow depth was measured visually from video recordings (25 frames/s). Each experiment was repeated three times and captured on video. The volume left on the chute after each experiment was calculated from the depth of the remaining fluid on the chute. The measurements are inaccurate for relatively little overtopping (estimated accuracy ±0.1 m^3).

A catching dam was located at the lower end of the chute. The different dam setups tested are listed in Table 2 and Table 1. Setup A comprises impermeable dams inclined at different angles to the chute (horizontal) between 34° and 100°. Setup C comprises permeable rock dams and/or rock berms. Setup B, entails experiments with mounds upstream of the impermeable dams in setup A.

Table 1 Setup B. Experimental setups of one and two rows of low obstacles (mounds and dams) upstream of an impermeable catching dam.

Setup no.	α_{mounds} (°)	α_{dam} (°)	No. of rows upstream	Description
B.1	90	90	1	One row of mounds + a steep catching dam (A.1)
B.2	90	90	2	Two rows of mounds + a steep catching dam (A.1)
B.3	90	75	1	1 row of mounds + 75° catching dam (A.2)
B.4	90	34	1	1 row of mounds + 34° catching dam (A.4)
B.5	90	90	1	1 low catching dam + vertical dam (A.1)
B.6	90	90	2	2 low catching dams + vertical dam (A.1)

Table 2 Setup A and C. Experimental setups for a single dam at the end of the experimental chute. The dam height is 1 m and H_{dam}/h_1 = 7–12. The rock berms and rock dams are 0.5 m thick and span the width of the chute.

Setup no.	α_{dam} (°)	Description
A.1	90	Vertical front face. Control experiment
A.2	75	Typical steep avalanche dam
A.3	60	Steep avalanche dam
A.4	34	Typical soil dam
A.5	95	Overhanging dam, *e.g.* harbour wall
A.6	100	Overhanging dam, *e.g.* harbour wall
C.1	90	1 m high, steep 0.5m thick rock dam, rocks fixed, no back plate (the dam is permeable)
C.2	33 + 90	0.5 m high, 33° berm of fixed rocks on a steep rock dam
C.3	33 + 90	0.5 m high, 33° berm of loose rocks on a steep rock dam
C.4	90	1 m high rock berm on a steep, impermeable dam face (A.1)
C.5	90	0.5 m high, steep rock dam.
C.6	90 + 90	0.5 m high rock berm on a steep, impermeable dam face (A.1)

4. ANALYSIS AND RESULTS

4.1 Chute flow: Experimental setup without obstacles upstream of the dam

The flow on the chute is turbulent and lasts for approximately 9 s. The front is thin, fast flowing and short, see Figure 4. The body of the flow is thicker and slower and remains semi-steady for approximately 1.5 s. The tail of the flow is decelerating and thinning for the remaining 5 to 8 s. The surface of the flow is irregular. The irregularities are characterized by two length scales, a larger scale (order of 1 m) and a smaller scale (order of 0.025 m).

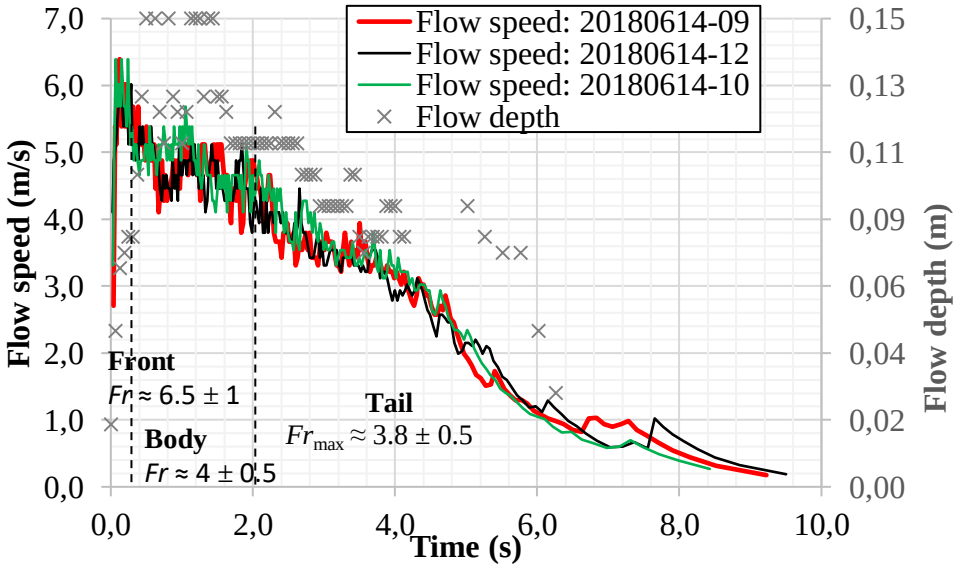

Figure 4 The flow speed and flow depth 0.5 m upstream of the catching dam as a function of time for 2.7 m^3 of water released from the tank and the experimental setup without obstacles upstream of the dam.

4.2 Impact with catching dams: Experimental setups A and C

Photographs of three distinct faces in the impact of the flow with an impermeable dam (setup A.1) and a permeable dam (setup C.1) are shown in Figure 5. Upon impacting the catching dam, the flow splashes high up on the dam face (Figure 5 A). This initial interaction is short lived, typically lasting just 0.06 s, which corresponds to one frame of the video recordings, although the evolution of the splash-up the dam face can be readily followed for 0.7 s. The jet then collapses upon the flow that is moving up the dam face. The run-up is then reduced and a semi-steady fountain that overflows the dam forms and prevails for approximately 1 s (Figure 5 B). These fountains resemble violent wave impacts on ocean walls following the initial splash (see Figure 2). Water continues to pile up at the dam face and the fountain collapses approximately 1.7 s after the initial impact. A hydraulic jump then forms in 0.2 s (Figure 5 C). Splashing over the dam is reduced but is present until the hydraulic jump has propagated approximately 2 m up the chute or over twice its width.

4.2.1 Setup A: Interpretation

The most effective impermeable dam setup in terms of the volume of overflow is setup A.6, with a steeper than vertical dam face. The least effective setup is A.4 with a dam face sloping at 1:1.5 (34° to the horizontal). No difference was observed in the depth of the hydraulic jump for the different setups.

4.2.2 Setup C: Interpretation

The most effective rock dam setup is setup C.1. Setup C.2 with a berm sloping at 34° is least effective and the only rock dam setup with overtopping. The rocks in the berm in setup C.3, become mobilized during the first two flow phases. The rocks had been arranged at the dam face, but were loose, as is common practice for ocean breakwaters. The rock size of 0.1–0.2 m is comparable to rocks of size 1–2 m in the field. Setups C.4 and C.6, with a 1 m and 0.5 m high, respectivly, steep, 0.5 m thick rock layer upstream of a dense, steep catching dam (A.1), yielded similar results as setup C.1.

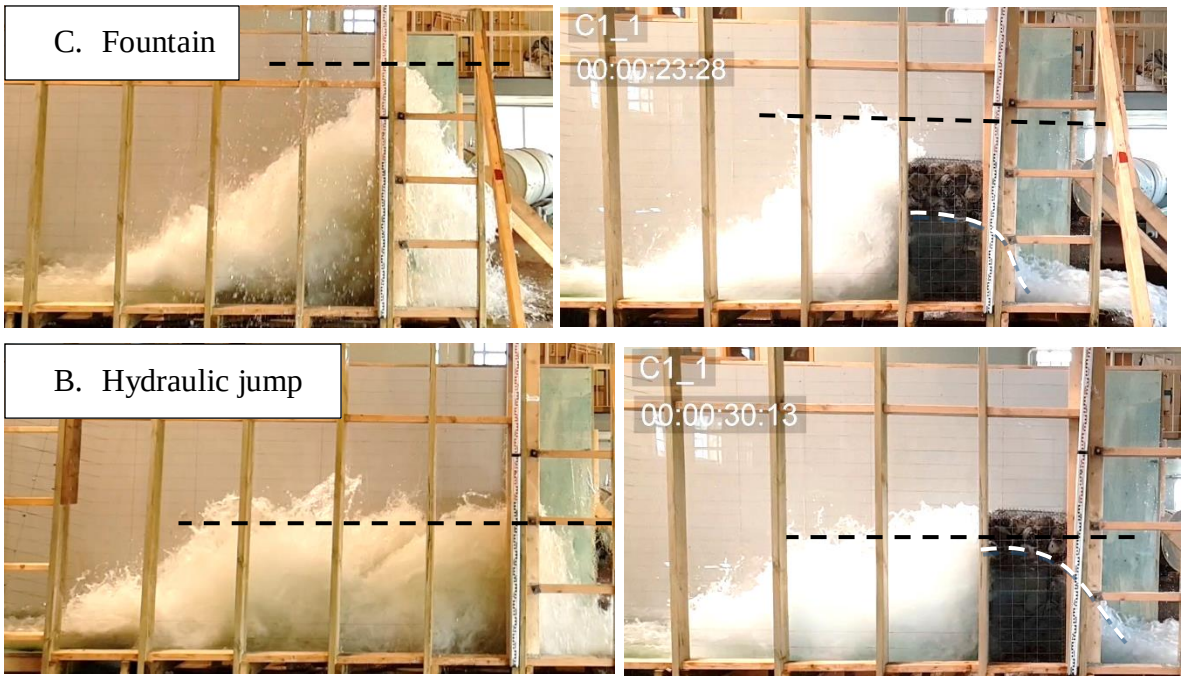

Figure 5 Experimental setup A.1 and C.1. The dashed black lines note the maximum run-up and the dashed white curves enhance the water table in the rockfill. The horizontal grid spacing on the chute is 0.1 m. **A.** Initial splash, approximately 0.6 s from impact. **B.** Fountaining, approximately 1.25 s from initial impact. **C.** Hydraulic jump, approximately 2 s from initial impact.

4.3 **Impact with combinations of mounds and catching dams: Experimental setup B**

Photographs of three distinct faces in the impact of the flow with two rows of small mounds upstream of an impermeable catching dam (Setup B.2) are shown in Figure 6. A high splash is observed upon the impact with the upper row of mounds. The splash is abrupt, and rises vertically for 0.6 s. The splash collapses over both rows of mounds and also partly upon the upward moving flow and a semi-steady jet is launched over the mounds. The jet lands upstream of the lower row of mounds. A splash is not observed at the lower row of mounds but a jet is formed, smaller than at the upper row. Neither a splash nor fountaining is observed at the face of the catching dam at the end of the chute. Rather a hydraulic jump is formed immediately after the impact.

4.3.1 Interpretation

Setup B.2, with two rows of breaking mounds upstream of the catching dam, is most effective and setup B.4 with a dam corresponding to a construction of loose materials is least effective. Setup B.1, with one row of mounds, is almost as effective as setup B.2 with two rows.

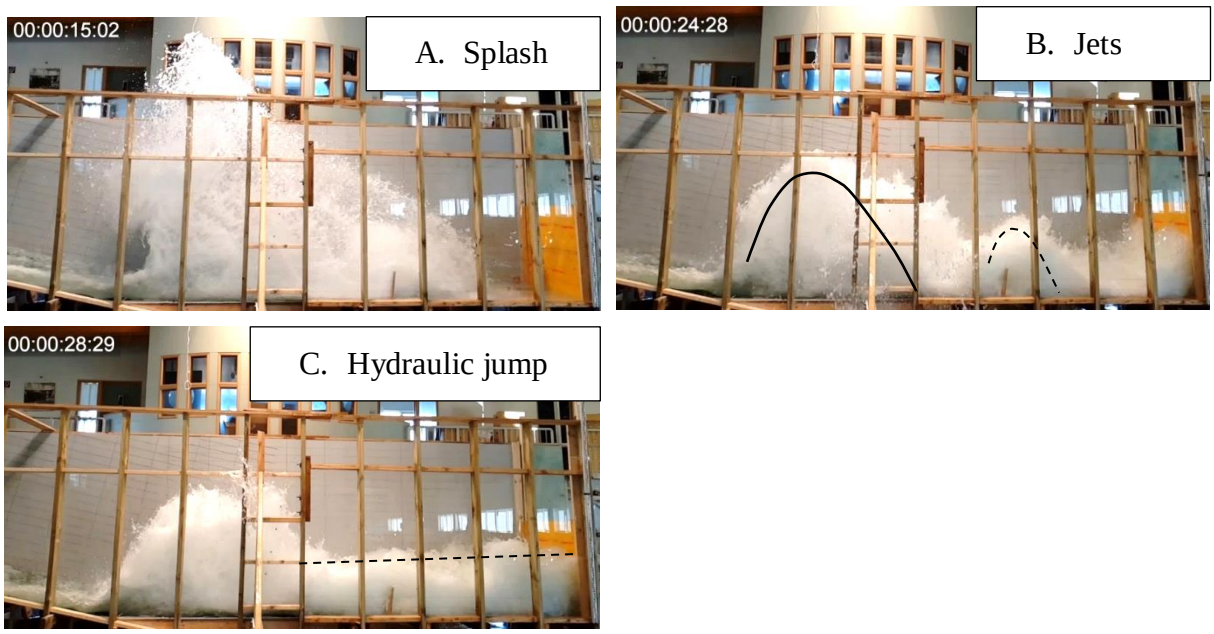

Figure 6 **A.** Initial splash, approximately 0.6 s after the initial impact (left). **B.** Semi-steady flow phase, approximately 2 s after the initial impact. The measured flow speed at the upper row of mounds is u_1 = 5,0 ± 0,25 m/s. The throw angle, θ is 67° and 71°, at the upper and lower row of mounds, respectively. **C.** Propagation of a hydraulic jump, approximately 2.5 s after the initial impact. The jump has caught up with the lower row of mounds.

5. CONCLUSIONS AND FURTHER STUDIES

The following main results have been observed in the impact of high-Froude number water flow and impermeable catching dams (experimental setup A):

- The initial impact with a dam is violent and a pressure-induced jet shoots up the dam face over twice as high as energy conservation would suggest. This phenomenon is also observed in violent wave impacts with harbour walls.
- The splash collapses after the initial impact and fountaining is observed prior to the onset of a hydraulic jump, approximately 2 s after the initial impact, or 6 s at the natural scale. Overtopping of the dam occurs during this period. The fountain height is comparable with the energy height if no energy is dissipated in the impact with the dam.
- Overtopping decreases with a steeper dam face and is eliminated in the case of a 100° dam face.
- Overtopping may also be reduced or eliminated by reducing the initial splash height at the dam face, with:
  - A row of steep mounds upstream of the dam.
  - A permeable steep rock dam or a steep rock berm at the upstream face of an impermeable dam.

- Impact forces are high enough to move 0.1–0.2 m wide rocks or 1–2 m boulders at the natural scale.

Many questions about the effective design of catching dams to contain slushflows remain unanswered and we raise a few of them here:

- Debris may pile up upstream of dams and mounds in an impact of a slushflow with such defence structures. If a second slushflow is released shortly after, the effectiveness of the protection measures may be reduced. The debris may form a ramp for a secondary release to shoot up.
- Wave-like instabilities or surges and roll waves have been observed in slushflows with Fr close to 1. Those may reduce the effectiveness of dams because of secondary impacts.
- The damping effect of a rock berm may depend on the width of the rock layer that water is ejected through. The width of the rock layer in the experiments was 0.50 m or (2.5–5) D, where D is the diameter of rocks.
- If the voids in a rock dam or a rock berm have filled with ice and snow over the winter, the rock dam will not dampen the initial impact. The slushflow may also fill the voids and reduce the damping effect.
- The observed mobilization of rocks in the berm in experiment C.3 indicates that erosion of mounds built from loose materials by rapidly moving slushflows may quickly reduce or eliminate their effect on the flow, even for large rock sizes. Erosion protection may be an important aspect of the design of slush flow protection measures of this type.

Previous laboratory studies on the impact of granular flows with obstacles, conducted at small length scales (1:100), show granular jumps upstream of catching dams, with a depth readily predicted from shallow-water theory. A substantial difference between granular flows and water flows is, however, observed in the first two impact phases (splash and fountaining):

- A granular splash is hardly observable.
- Fountaining is not observed.
- The transition from the initial impact to a granular jump happens almost instantly, or much more quickly than in water flows.

This difference is ascribed to a dilute flow front of the granular flows that is able to compress considerably, whereas water is incompressible (Hákonardóttir and Hogg, 2005). A difference is also observed regarding energy dissipation in the impact with mounds. In granular impacts, a considerable dissipation of energy occurs at the mound face (Hákonardóttir et al., 2003b, 2003c), which is not observed in water impacts. The mixing of streams from individual mounds and the turbulence during the landing on the chute may account for the dissipation of the energy in the water flows. Air drag may add further to the dissipation at larger scales (Jóhannesson et al., 2009).

ACKNOWLEDGEMENTS

The authors would like to acknowledge the financial support of the Icelandic Avalanche Fund and thank the following people: Tómas Jóhannesson of the Icelandic Meteorological Office for his review, active collaboration and support at all stages of the work. Sigurður Sigurðarson of the Icelandic Road and Coastal Administration for his insight into the design of breakwaters and wave experiments. The active support of the staff at the Coastal Administration laboratory.

Van der Meer of Van der Meer Consulting B.V. for reviewing the design of the slushflow simulator and his visit during the design stage. Hafþór Örn Pétursson mechanical engineer at Verkís, for the design of the simulator. Halldór Pálsson and Ásdís Helgadóttir at the Faculty of Industrial Engineering, Mechanical Engineering and Computer Science at the University of Iceland for the collaboration and support.

REFERENCES

Ágústsson, K., Jóhannesson, T., Sauermoser, S., Sigurðsson, H.Þ., 2003a. *Hazard zoning for Patreksfjörður, Vesturbyggð*. Report 03029. The Icelandic Meteorological Office.

Ágústsson, K., Jóhannesson, T., Sauermoser, S., Sigurðsson, H.Þ., Jenson, E.H., 2003b. *Hazard zoning for Bíldudalur, Vesturbyggð*. Report 03034. The Icelandic Meteorological Office.

Bruce, T., van der Meer, J.W., Franco, L., Pearson, J.M. 2009. Overtopping performance of different armour units for rubble mound breakwaters. *Coastal Engineering*, 56, 166–179.

Brennen, C.E., Sieck, K., Paslaski, J., 1983. Hydraulic jumps in granular material flow. *Powder Technol.*, 35, 31–37.

Cooker, J.M., Peregrine, D.H., 1995. Pressure-impulse theory for liquid impact problems. *J. Fluid Mech*., 297, 193–214.

Gauer, P., 2004. Numerical modelling of a slushflow event. In: *Proceedings of ISSW-2004*, 39–43.

Gray, J. M. N. T., Tai, Y.-C., and Noelle, S., 2003. Shock waves, dead-zones and particle-free regions in rapid granular free surface flows. *J. Fluid Mech.*, 491, 161–181.

Gude, M., Scherer, D., 1998. Snowmelt and slushflows: hydrological and hazard implications. *Ann. Glaciol.*, 26, 381–384.

Hager,W.H., 1992. *Energy Dissipators and Hydraulic Jump*. Kluwer Academic Publishers.

Hákonardóttir, K.M., Hogg, A.J., Batey, J., Woods, A.W., 2003a. Flying avalanches. *Geophysical Research Letters*, 30(23), 20191.

Hákonardóttir, K.M., Hogg, A.J., Jóhannesson, T., Tómasson, G.G., 2003b. A laboratory study of the retarding effect of braking mounds on snow avalanches. J. *Glaciol.*, 49(165), 191–200.

Hákonardóttir, K. M., Hogg, A. J., Jóhannesson, T., Kern, M. og Tiefenbacher, F., 2003c. Large-scale avalanches braking mound and catching dam experiments with snow: A study of the airborne jet. *Surveys in Geophysics*, 24(5–6), 543–554.

Hákonardóttir, K.M., Hogg, A.J., 2005. Oblique shocks in rapid granular flows. *Physics of Fluids*, 17, 077101, doi: 10.1063/1.1950688.

Hestnes, E., 1985. A contribution to the prediction of slush avalanches. *Ann. Glaciol*., 6, 1–4.

Hestnes, E. 1998. Slushflow hazard – where, why and when? *25 years of experience with slushflow consulting and research*. Ann. Glaciol., 26, 370–376.

Hestnes, E., Bakkehöi, S., Kristensen, K., 2011. Slushflows – A challenging problem to authorities and experts. In: *Proceedings of the Int. Conf. on Avalanches and Related Subjects, September 5–9, 2010*, Production association “Apatit”, Kirovsk, Murmansk Region, Russia.

Hestnes, E., Kristensen, K., 2011. The diversities of large slushflows illustrated by selected cases. In: *Proceedings of the Int. Conf. on Avalanches and Related Subjects, September 5–9, 2010*, Production association “Apatit”, Kirovsk, Murmansk Region, Russia.

Hestnes, E., Sandersen, F., 2000. The main principles of slushflow hazard mitigation. In: *Proceedings of the INTERPRAEVENT 2000*, Villach, Austria. Tagungspublikation 2, 267–280.

Issler, D., 2003. Experimental information on the dynamics of dry-snow avalanches. In: Hutter, K., Kirchner, N. (eds.), *Dynamic Response of Granular and Porous Materials under Large and Catastrophic Deformations*. Springer Berlin, 109–160.

Jaedicke, C., Kern, M., Gauer, P., Baillifard, M.-A., Platzer, K., 2008. Chute experiments on slushflow dynamics. *Cold Regions Science and Technology*, 51, 156–167.

Jóhannesson, T., Gauer, P., Issler, D, Lied, K., (eds.), 2009. *The design of avalanche protection dams. Recent practical and theoretical developments*. Brussels, Directorate-General for Research, Environment Directorate, European Commission, Publication EUR 23339, 195 pp., doi: 10.2777/12871.

Jóhannesson, T., Hákonardóttir, K.M., 2004. *Töluleg hermun á krapaflóði úr Geirseyrargili á Patreksfirði: Samantekt niðurstaðna (A numerical simulation of a slushflow from Geirseyrargil Patreksfjörður: Summary of results)*. The Icelandic Meteorological Office. Memo VS-KMH-2004-01.

Margreth, S., 2015. *Analysis of the hazard situation and the proposed mitigation measures in Patreksfjörður and Bíldudalur, Iceland*. SLF Expert Report G2015.21, 23 pp.

Najafi-Jilani, A., Monshizadeh, M., 2010. Laboratory Investigations on Wave Run-up and Transmission over Breakwaters Covered by Antifer Units. Transaction A: *Civil Engineering*, 17(6), 457–470.

Peterka, A.J., 1984. *Hydraulic design of stilling basins and energy dissipators*. Engineering Monograph, 25. Denver, US Department of the Interior, US Bureau of Reclamation.

Rudolf-Miklau, F., Sauermoser, S., Mears, A., eds. 2015. *The Technical Avalanche Protection Handbook*. John Wiley & Sons, 430 pp.

Salm, B., Burkard, A., Gubler, H. U., 1990. *Berechnung von Fliesslawinen. Eine Anleitung fuer Praktiker mit Bleispielen*. Davos, Eidgenössisches Institut für Schnee- und Lawinenforschung, Mitteilungen Nr. 47.

Savage, S.B., 1979. Gravity flow of cohesionless granular materials in chutes and channels. *J. Fluid Mech*. 92, 53–96.

Sigurðsson, F., Tómasson, G.G., Hestnes, E., 1998. Vesturbyggð. *Slushflow defences. Appraisal for Geirseyrargil*. Report VST: 97.206, NGI: 974063.

Sovilla, B., Sonatore, I., Bühler, Y., Margreth, S., 2012. Wet-snow avalanche interaction with a deflecting dam: field observations and numerical simulations in a case study. *Nat. Hazards Earth Syst. Sci*., 12, 1407–1423.

Upadhyay, A., Kumar, A., Chaudhary, A., 2010. Velocity measurements of wet snow avalanches on the Dhundi snow chute. *Ann. of Glaciol*. 51(54), 139–145.

Van der Meer, J., Sigurðarson, S., 2017. *Design and construction of berm breakwaters*. World Scientific, 329 pp.